ISBN: 978-3-95450-261-5 ISSN: 2673-7000 doi: 10.18429/JACoW-NAPAC2025-TUP030

DENSITY FUNCTIONAL THEORY APPROACH FOR CALCULATING ELECTRONIC BAND STRUCTURE PARAMETERS FOR MONTE CARLO SIMULATIONS OF PHOTOEMISSION

J. O. Mendez*, J. Callahan, O. Chubenko, Northern Illinois University, DeKalb, IL, USA
L. Cultrera, Brookhaven National Laboratory, Upton, NY, USA
S. Karkare, Arizona State University, Tempe, AZ, USA
R. Palai, University of Puerto Rico Rio Piedras, San Juan, PR, USA

Abstract

Monte Carlo simulations are a powerful tool for modeling photoemission from photocathodes, enabling the prediction of key parameters, such as quantum efficiency, mean transverse energy, electron spin polarization, and photocathode response time. However, these simulations require material band structure parameters, which are not always available from experiments. This work aims to establish a reliable framework for calculating electronic band structure parameters using Density Functional Theory (DFT). Specifically, we apply this framework to investigate the effects of lattice strain and temperature on the electronic band structure and electron transport in GaAs. This approach will be further extended to explore band structure modifications in heavily *p*-doped semiconductors and to calculate electronic band structures of novel spin-polarized photocathode materials.

INTRODUCTION

GaAs based photocathodes are widely used in accelerator science due to their ability to produce spin-polarized electrons with high brightness. While strained superlattices [1] can enhance polarization, their quantum efficiency (QE) is often reduced and fabrication is costly. Moreover, activation with cesium remains necessary and vulnerable to ion bombardment. The search for alternative materials and structures with improved properties is ongoing [2–5], but experimental investigations remain time-intensive.

Computational modeling, particularly density functional theory (DFT) in combination with Monte Carlo (MC) simulations, offers a cost-effective and quick method to explore new materials under different operating conditions for advanced photocathodes. The goal of this work is to develop a robust framework in which temperature and strain dependent material parameters derived from DFT can be reliably used in MC simulations [6] of electron transport and photoemission. We use bulk GaAs as a benchmark material due to the availability of extensive experimental data.

METHODS

Electronic structure calculations were performed using Quantum ESPRESSO with fully relativistic norm-conserving pseudopotentials and with Perdew Burke Erzenhof (PBE) exchange-correlation functional [7–9]. To address the known underestimation of the GaAs band gap from DFT [10, 11], we employed the DFT+U correction method, tuning the Hubbard U parameter to reproduce an intrinsic band gap of 1.52 eV at 2 K [12], and up to 1.42 eV at room temperature (293 K) [12]. The procedure for testing different values of U involved calculating the electronic band gap energy as well as the static and high frequency dielectric constants. The U was applied to the arsenic ranging from 0 eV to 10 eV in steps of 0.5 eV, and for gallium the range was from 0 eV to 20 eV with the same step value. Applying the U to arsenic resulted in greater change of the parameters than applying it to Gallium. Figures 1 and 2 demonstrate how choosing a U value that provides good agreement for all parameters might be difficult as each parameter is affected differently by the Hubbard correction. Ultimately, the above-mentioned approach of applying different values of U for different temperatures only to arsenic was chosen to ensure that the intrinsic band gap closely matches the value given by the equation $E_g = 1.522 - 5.8 \times 10^{-4}(\frac{T^2}{T+300})$ [12].

Temperature effects were incorporated via thermal expansion coefficient using experimentally measured coefficients, while strain was modeled by transforming the zincblende unit cell to an orthorhombic face centered to emulate pseudomorphic growth under biaxial compression. From these calculations, we extracted effective masses, non-parabolicity factors, static and high frequency dielectrics, phonon dispersion, and optical transmission and reflectivity as a function of temperature and strain. These parameters were used in a spin-resolved MC transport model [6] simulating drift velocity as a function of electric field strength. The model includes scattering and spin-relaxation effects essential to spin-polarized photoemission.

RESULTS

Tables 1 and 2 summarize the results from the DFT calculations. The parameter that is closest to their reference value is the intrinsic band gap due to the applied Hubbard Correction (Fig. 3). The calculated band gap increases with applied in-plane compressive strain, rising from 1.42 eV to 1.55 eV at −5.0 % strain, which can be observed in Fig. 4. Additionally the loss of degeneracy of the light and heavy hole bands due to the strain was able to be observed with the strain, and not at different temperatures as seen in Fig. 3. Experimental data for the high frequency dielectric constant show that it increases as the temperature increases [13]. We observed this trend in the DFT results when the the Hubbard correction was not applied or when it was not change for every temperature.

* z2044141@students.niu.edu

ISBN: 978-3-95450-261-5 ISSN: 2673-7000 doi: 10.18429/JACoW-NAPAC2025-TUP030

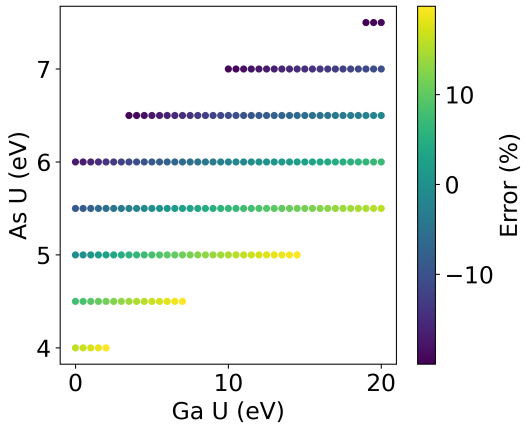

Figure 1: Band gap error (%) as a function of Hubbard U values applied to Ga and As in GaAs at 293 K. The x-axis represents the U applied to Ga, and the y-axis to As. The color indicates the percentage error in the calculated band gap relative to Ref. [12]. Only includes values where $|error| < 20\,\%$.

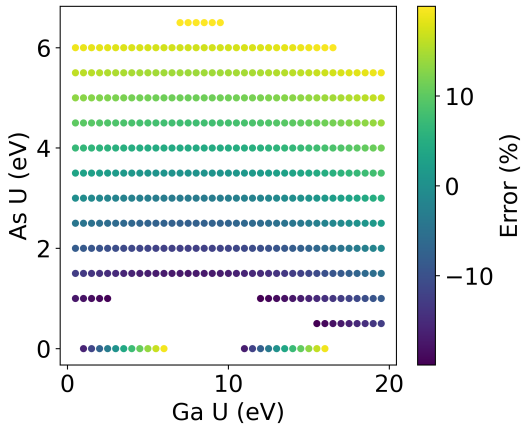

Figure 2: Same as Fig. 1 but for the error of the high frequency dielectric constant compared to that in Ref. [13].

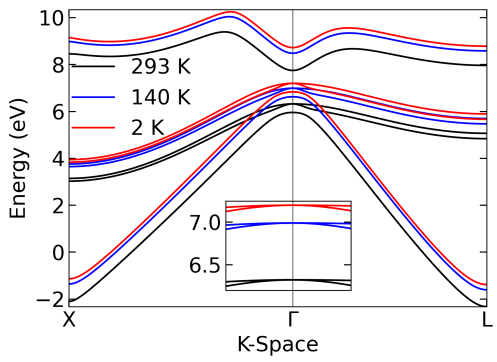

Figure 3: The calculated band structure for GaAs from DFT for the path $X \rightarrow \Gamma \rightarrow L$ at 2 K, 140 K, and 293 K.

Table 1: Parameters of GaAs at 2 K, 77 K, and 293 K From DFT Results (the set of reference experimental values at 293 K [6] is shown for comparison)

Parameters	2 K	77 K	293 K	293 K [6]
Effective Mass (m_g)				
Split off	0.1791	0.1786	0.1750	0.14
Light Hole	0.0960	0.0955	0.0909	0.088
Heavy Hole	0.3096	0.3102	0.3261	0.51
CB - Γ	0.0792	0.0788	0.0748	0.063
CB - X	0.4759	0.4825	0.2025	0.58
CB - L	0.2917	0.2927	0.3316	0.22
Energy Gaps (eV)				
Intrinsic	1.525	1.513	1.426	1.42
L	1.584	1.580	1.640	1.71
X	1.949	1.951	2.135	1.9
Split Off	0.3637	0.3636	0.3658	0.34
Band Splitting Energy (eV)				
CB - L	0.0592	0.0668	0.2147	0.29
CB - X	0.4240	0.4378	0.7090	0.48
Optical Parameters				
h.f. dielectric	10.18	10.19	9.81	10.92
static dielectric	12.39	12.42	12.66	12.9

Table 2: Parameters of GaAs With −0.5 %, −1.0 %, and −5.0 % Strain From DFT Results (the set of reference experimental values at 293 K with 0 % strain [6] is shown for comparison)

Parameters	−0.5 %	−1.0 %	−5.0 %	0 % [6]
Effective Mass (m_0)				
Split off	0.1529	0.1373	0.0956	0.14
Light Hole	0.0991	0.1128	0.2551	0.088
Heavy Hole	0.3169	0.3167	0.2991	0.51
CB - Γ	0.0757	0.0785	0.0920	0.063
CB - X	0.1949	0.2881	0.2609	0.58
CB - Z	0.1907	0.2043	0.2488	0.58
CB - L	0.3185	0.3097	0.2537	0.22
Energy Gaps (eV)				
Intrinsic	1.447	1.467	1.554	1.42
L	1.637	1.630	1.406	1.71
X	2.081	2.027	1.557	1.9
Z	2.180	2.225	2.451	1.9
Split Off	0.351	0.345	0.688	0.34
Band Splitting Energy (eV)				
CB - L	0.1897	0.1625	0.1478	0.29
CB - X	0.6340	0.5598	0.0038	0.48
CB - Z	0.7324	0.7573	0.8975	0.48
Holes	0.038	0.072	0.201	0.0
Optical Parameters				
h.f. dielectric	9.74	9.67	9.39	10.92
static dielectric	12.50	12.36	11.61	12.9

Monte Carlo simulations using calculated DFT parameters from Table 1 predict drift velocity trends consistent with experimental data [14], but with quantitative discrepancies at low field strengths as seen in Fig. 5. By correcting three

ISBN: 978-3-95450-261-5 ISSN: 2673-7000 doi: 10.18429/JACoW-NAPAC2025-TUP030

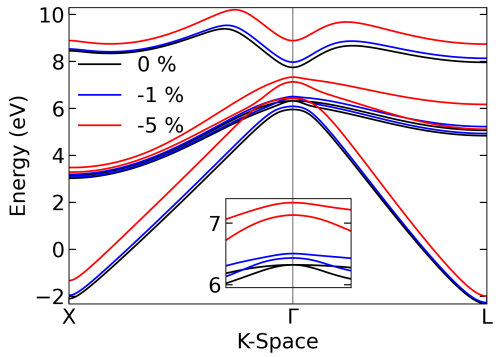

Figure 4: The calculated band structure for GaAs from DFT for the path $X \rightarrow \Gamma \rightarrow L$ at 0 %, −1 %, and −5 % strain.

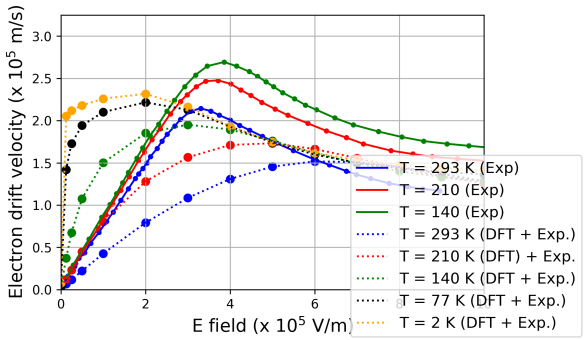

Figure 5: The MC electron drift velocity as a function of applied electric field using the DFT calculations for various temperatures compared to experiment [14].

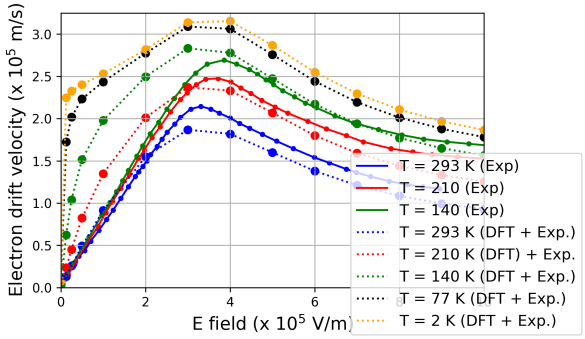

Figure 6: Same as Fig. 5 but after applying a correction to the results of the DFT calculations at different temperatures.

key parameters (Γ-valley effective mass, $\Gamma - L$ splitting, and high frequency dielectric constant) to match experimental values at 293 K, the agreement with drift velocity [14] and mobility measurements [15] significantly improved (Figs. 6 and 7). These corrections were applied systematically as multiplicative coefficients across all temperature and strain levels studied in this work (Fig. 8). Results showed that this hybrid approach yields accurate electron mobility and drift velocity predictions across the studied range, reinforcing the critical influence of these three parameters on transport simulations.

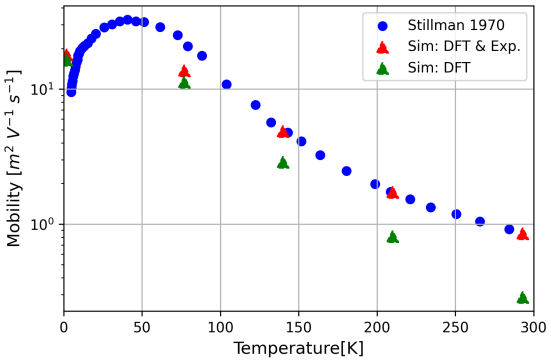

Figure 7: The MC mobility as a function of temperature before (green) and after (red) applying a correction to the results of the DFT calculations compared to experiment [15].

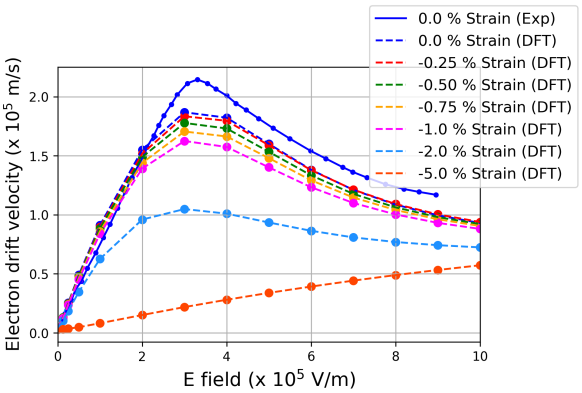

Figure 8: The MC electron drift velocity as a function of applied electric field after applying a correction to the results of the DFT calculations for different amount of strains.

CONCLUSION

This work demonstrates that DFT can be effectively used to model the effects of strain and temperature on the electronic structure and transport properties of GaAs when validated and calibrated against experimental benchmarks. The sensitivity of drift velocity and mobility to a few specific parameters underscores the importance of calibration in multiscale modeling.

ACKNOWLEDGMENTS

This work was performed under the Chicagoland Accelerator Science Traineeship (CAST) program sponsored by the U.S. DOE award DE-SC0020379 to the Illinois Institute of Technology (IIT) and Northern Illinois University (NIU). This work used resources of the Center for Research Computing and Data at NIU. J. O. M. and L. C. were supported by Brookhaven Science Associates, LLC under Contract DE-SC0012704 with the U.S. DOE. O. C. and S. K. were supported by the U.S. National Science Foundation under Award PHY-1549132, the Center for Bright Beams. R. P. acknowledges the financial support received from the DoE through the SPINS Consortium, Grant # DE-NA0003980.

ISBN: 978-3-95450-261-5 ISSN: 2673-7000 doi: 10.18429/JACoW-NAPAC2025-TUP030

REFERENCES

[1] W. Liu *et al.*, "Record-level quantum efficiency from a high polarization strained GaAs/GaAsP superlattice photocathode with distributed bragg reflector", *Appl. Phys. Lett.*, vol. 109, no. 25, p. 252 104, 2016. doi:10.1063/1.4972180

[2] J. Marini, I. Mahaboob, E. Rocco, L. Bell, and F. Shahedipour-Sandvik, "Polarization engineered N-polar Cs-free GaN photocathodes", *J. Appl. Phys.*, vol. 124, no. 11, p. 113 101, 2018. doi:10.1063/1.5029975

[3] L. Cultrera *et al.*, "Photoemission characterization of N-polar III-nitride photocathodes as candidate bright electron beam sources for accelerator applications", *J. Appl. Phys.*, vol. 131, no. 12, p. 124 902, 2022. doi:10.1063/5.0076488

[4] J. K. Bae, A. Galdi, L. Cultrera, F. Ikponmwen, J. Maxson, and I. Bazarov, "Improved lifetime of a high spin polarization superlattice photocathode", *J. Appl. Phys.*, vol. 127, no. 12, p. 124 901, 2020. doi:10.1063/1.5139674

[5] V. Rusetsky *et al.*, "New spin-polarized electron source based on alkali antimonide photocathode", *Phys. Rev. Lett.*, vol. 129, no. 16, p. 166 802, 2022. doi:10.1103/PhysRevLett.129.166802

[6] O. Chubenko *et al.*, "Monte carlo modeling of spin-polarized photoemission from p-doped bulk GaAs", *J. Appl. Phys.*, vol. 130, no. 6, p. 063 101, 2021. doi:10.1063/5.0060151

[7] P. Giannozzi *et al.*, "QUANTUM ESPRESSO: A modular and open-source software project for quantum simulations of materials", *J. Phys.: Condens. Matter*, vol. 21, no. 39, p. 395 502, 2009. doi:10.1088/0953-8984/21/39/395502

[8] P. Giannozzi *et al.*, "Advanced capabilities for materials modelling with quantum espresso", *J. Phys.: Condens. Matter*, vol. 29, no. 46, p. 465 901, 2017. doi:10.1088/1361-648X/aa8f79

[9] D. R. Hamann, "Optimized norm-conserving vanderbilt pseudopotentials", *Phys. Rev. B*, vol. 88, no. 8, 2013. doi:10.1103/PhysRevB.88.085117

[10] J. P. Perdew and M. Levy, "Physical content of the exact Kohn-Sham orbital energies: Band gaps and derivative discontinuities", *Phys. Rev. Lett.*, vol. 51, no. 20, pp. 1884–1887, 1983. doi:10.1103/PhysRevLett.51.1884

[11] L. J. Sham and M. Schlüter, "Density-functional theory of the energy gap", *Phys. Rev. Lett.*, vol. 51, no. 20, pp. 1888–1891, 1983. doi:10.1103/PhysRevLett.51.1888

[12] M. B. Panish and J. Casey H. C., "Temperature dependence of the energy gap in GaAs and GaP", *J. Appl. Phys.*, vol. 40, no. 1, pp. 163–167, 1969. doi:10.1063/1.1657024

[13] I. Strzalkowski, S. Joshi, and C. R. Crowell, "Dielectric constant and its temperature dependence for GaAs, CdTe, and ZnSe", *Appl. Phys. Lett.*, vol. 28, no. 6, pp. 350–352, 1976. doi:10.1063/1.88755

[14] J. G. Ruch and G. S. Kino, "Transport properties of GaAs", *Phys. Rev.*, vol. 174, no. 3, pp. 921–931, 1968. doi:10.1103/PhysRev.174.921

[15] G. E. Stillman, C. M. Wolfe, and O. Dimmock J, "Hall coefficient factor for polar mode scattering in n-type GaAs", *Journal Phys. Chem. Solids*, vol. 31, no. 6, pp. 1199–1204, 1970. doi:10.1016/0022-3697(70)90122-8